Biochemistry

 Volume 33, Number 21 May 31, 1994

Articles

The Chloroperoxidase-Catalyzed Oxidation of Phenols. Mechanism, Selectivity, and Characterization of Enzyme–Substrate Complexes†

Luigi Casella*

Dipartimento di Chimica Generale, Università di Pavia, 27100 Pavia, Italy

Sonia Poli, Michele Gullotti, Carlo Selvaggini, and Tiziana Beringhelli

Dipartimento di Chimica Inorganica, Metallorganica e Analitica, Centro CNR, Università di Milano, 20133 Milano, Italy

Augusto Marchesini

Istituto per la Nutrizione delle Piante, Sezione di Torino, Via Ormea 47, 10125 Torino, Italy

Received November 24, 1993; Revised Manuscript Received February 23, 1994®

ABSTRACT: The reactivity of a series of *para*-substituted phenolic compounds in the peroxidation catalyzed by chloroperoxidase was investigated, and the results were interpreted on the basis of the binding characteristics of the substrates to the active site of the enzyme. Marked selectivity effects are observed. These operate through charge, preventing phenolic compounds carrying amino groups on the substituent chain to act as substrates for the enzyme, and through size, excluding potential substrates containing bulky substituents to the phenol nucleus. Also, chiral recognition is exhibited by chloroperoxidase in the oxidation of *N*-acetyltyrosine, where only the L isomer is oxidized. Kinetic measurements show that, in general, the efficiency of chloroperoxidase in the oxidation of phenols is lower than that of horseradish peroxidase. Paramagnetic NMR spectra and relaxation rate measurements of chloroperoxidase–phenol complexes are consistent with binding of the substrates close to the heme, in the distal pocket, with the phenol group pointing toward the iron atom. On the other hand, phenolic compounds which are not substrates for chloroperoxidase bind to the enzyme with a much different disposition, with the phenol group very distant from the iron and probably actually outside the active-site cavity.

Chloroperoxidase (chloride:hydrogen–peroxide oxidoreductase, EC 1.11.1.10)[1] is a rather versatile enzyme since it can catalyze classical reactions of peroxidases (Thomas et al., 1970), catalatic type reactions (Thomas et al., 1970a; Araiso et al., 1981), oxygen-transfer reactions (from H_2O_2) that are more typical of cytochrome P-450 (McCarthy & White, 1983; Ortiz de Montellano et al., 1987; Geigert et al., 1986), and halide ion-dependent halogenations of a variety of substrates (Hager et al., 1966; Libby et al., 1982; Itahara & Ide, 1987; Itoh et al., 1987; Griffin, 1991). This versatility depends on the particular structure of the active site of the enzyme, with a cysteine thiolate as the heme axial ligand (Blanke & Hager, 1989), as in P-450 (Poulos, 1987), and a polar heme environment, including a distal histidine residue, two asparagines (Blanke & Hager, 1990), and an arginine (Dugad et al., 1992), which render it more similar to that of common peroxidases (Sono et al., 1986; Dawson, 1988). We have recently found that CPO catalyzes the oxidation of organic sulfides to sulfoxides (Colonna et al., 1990, 1992; Casella et al., 1992) and the epoxidation of styrenes (Colonna et al.,

† Supported by the Progetto Finalizzato-Chimica Fine II of the Italian CNR.

® Abstract published in *Advance ACS Abstracts*, April 1, 1994.

[1] Abbreviations: CPO, chloroperoxidase; HRP, horseradish peroxidase; LPO, lactoperoxidase; P-450, cytochrome P-450; NMR, nuclear magnetic resonance.

0006-2960/94/0433-6377$04.50/0

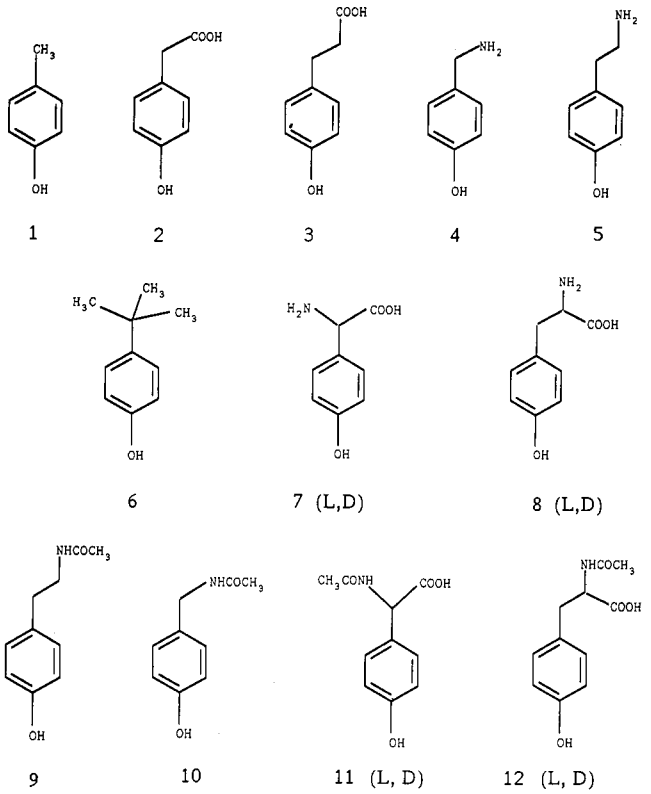

FIGURE 1: Phenolic compounds studied in the CPO- and HRP-catalyzed oxidation by hydrogen peroxide.

1993) by peroxides with high enantioselectivity [the latter reaction has been reported independently by Allain et al. (1993)], and we wish to report here on the marked selectivity effects exhibited by CPO in the catalytic oxidation of phenols by hydrogen peroxide.

Phenols are typical substrates for peroxidases (Dunford & Stillman, 1976; Frew & Jones, 1984; Dunford & Adeniran, 1986; Sakurada et al., 1990), but only scattered studies are available for the CPO-catalyzed oxidation of this class of compounds (Lambeir et al., 1987). In the attempt to extend our studies on the interaction of peroxidases with the L and D isomers of tyrosine (Casella et al., 1991), which are substrates for these enzymes in reactions occurring with interesting stereoselective effects (Bayse et al., 1972), we surprisingly found that the two tyrosine isomers are not oxidized by CPO in the presence of hydrogen peroxide. We thus decided to investigate the catalytic activity of CPO on a series of substituted phenols to establish the eventual existence of restrictions to reactivity due to steric effects or the presence of polar groups in the substrate structure. The phenolic compounds investigated are reported in Figure 1. The behavior of CPO toward these molecules is compared here with that of HRP. In order to explain the origin of the selectivity exhibited by CPO, the binding characteristics of several phenolic compounds to the enzyme have been investigated by spectroscopic techniques and NMR relaxation measurements. This information is already available for phenol binding to HRP (Sakurada et al., 1986; Casella et al., 1991).

MATERIALS AND METHODS

Materials. Chloroperoxidase was obtained from Sigma Chemical Co. as a suspension in 0.1 M sodium phosphate, pH 4, RZ = 1.0. It was further purified by ion-exchange chromatography on a CMC Sephadex column, by elution with a linear gradient of phosphate buffer, pH 4.0, from 10 to 100 mM. The RZ of the resulting enzyme solution was raised to 1.3. Horseradish peroxidase (mostly isoenzyme C) was obtained from Sigma Chemical Co. as a freeze-dried powder (type VI, RZ = 3.2 at pH 7.0). The concentrations of enzyme solutions were determined optically using ϵ_{400} 91 mM^{-1} cm^{-1} for CPO and ϵ_{403} 102 mM^{-1} cm^{-1} for HRP. The phenolic compounds *p*-cresol (**1**), *p*-hydroxyphenylacetic acid (**2**), (*p*-hydroxyphenyl)propionic acid (**3**), tyramine (**5**), *p*-*tert*-butylphenol (**6**), D- and L-(*p*-hydroxyphenyl)glycine (D-**7** and L-**7**), D- and L-tyrosine (D-**8** and L-**8**), and *N*-acetyl-L-tyrosine (L-**12**) were available from commercial sources. *N*-acetyltyramine (**9**), *N*-acetyl-D-tyrosine (D-**12**), *N*-acetyl-L- and *N*-acetyl-D-(*p*-hydroxyphenyl)glycine (L-**11** and D-**11**), and *N*-acetyl-*p*-hydroxybenzylamine (**10**) were prepared by acetylation of the amine precursors following a literature procedure (Greenstein & Winitz, 1961). *p*-Hydroxybenzylamine (**4**) was prepared by reduction of *p*-hydroxybenzonitrile with lithium aluminum hydride in tetrahydrofuran and used as the crystalline oxalate derivative. The other reagents were of the highest grade available and used as received. All buffer solutions employed for the enzymatic studies were prepared from water purified by a Milli-Q purification system.

Kinetic Measurements. All kinetic measurements were done in 0.1 M acetate buffer, pH 5.0, at 20 ± 0.1 °C. The reactions were followed with a diode array HP-8452A single-beam spectrophotometer by measuring the increase in absorbance at 300 nm due to the phenol oxidative coupling dimers which form in the initial phase of the reaction. The reactions were started by adding fixed amounts of hydrogen peroxide to a 1-cm path length quartz cell containing the enzyme and variable quantities of the substrates to a fixed final volume of solution (2 mL). The following substrate and enzyme concentrations were used in the kinetic experiments. For CPO-catalyzed reactions: *p*-cresol 0–14.0 mM, CPO 7.3 nM; *p*-hydroxyphenylacetic acid 0–10.0 mM, CPO 15 nM; (*p*-hydroxyphenyl)propionic acid 0–25.0 mM, CPO 0.15 μM; *N*-acetyltyramine 0–30.0 mM, CPO 26 nM; *N*-acetyl-L-tyrosine 0–56.0 mM, CPO 0.4 μM. For HRP-catalyzed reactions: *p*-cresol 0–4.5 mM, HRP 8.7 nM; *p*-hydroxyphenylacetic acid 0–18.0 mM, HRP 20 nM; (*p*-hydroxyphenyl)-propionic acid 0–3.0 mM, HRP 6.7 nM; *N*-acetyltyramine 0–5.0 mM, HRP 11.0 nM; *N*-acetyl-L-tyrosine 0–28.0 mM, HRP 25.0 nM; *N*-acetyl-D-tyrosine 0–19.0 mM, HRP 25.0 nM. The concentration of hydrogen peroxide was 0.4 mM in all reactions catalyzed by HRP, while it had to be varied with the substrate when the catalyst was CPO: 5.0 mM with *p*-cresol, 1.0 mM with (*p*-hydroxyphenyl)propionic acid, and 0.5 mM with *p*-hydroxyphenylacetic acid, *N*-acetyltyramine, and *N*-acetyl-L-tyrosine.

In separate sets of experiments with CPO, hydrogen peroxide was the substrate considered, and its concentration was varied between 0 and 5 mM, while the concentration of phenolic substrate was kept constant as follows: *p*-cresol 10 mM, *p*-hydroxyphenylacetic acid 8 mM, (*p*-hydroxyphenyl)propionic acid 33 mM; CPO concentration was 16 nM.

The initial rates were determined from the linear part of the trace at 300 nm. All kinetic constants were determined from nonlinear least-squares fits of primary kinetic data to the Michaelis–Menten equation. To convert rates from absorbance/time into mol/time, a molar extinction coefficient (ϵ_{mix}) which reflects the composition of the product mixture was used. The ϵ_{mix} was determined from a plot of absorbance versus number of moles of hydrogen peroxide consumed in HRP-catalyzed reactions where hydrogen peroxide was the limiting reagent. The other conditions were the same as in

the kinetic experiments. A similar procedure was followed by Libby et al. (1989) in the analysis of the kinetic data for the CPO-catalyzed peroxidation of catechol, but apparently the catalatic activity of this enzyme was not considered. The rectilinear plot obtained in each series of experiments ensured that the composition of the product mixture was constant in all measurements. The following values (M^{-1} cm^{-1}) of ϵ_{mix} at 300 nm were obtained, 2350 for the oxidation products of *p*-cresol, 2100 for those of *p*-hydroxyphenylacetic acid, 2180 for those of (*p*-hydroxyphenyl)propionic acid, 1800 for those of *N*-acetyltyramine, and 1900 for those of *N*-acetyl-L- or -D-tyrosine. For comparison purposes, the values of ϵ_{mix} were determined also employing CPO as catalyst in the same conditions of the kinetics measurements, with hydrogen peroxide as limiting reagent.

Catalatic Activity. Determination of catalatic activity in the CPO reactions was performed by means of a Clark oxygen electrode, through the measurement of the dioxygen evolved in the solution by dismutation of hydrogen peroxide. The reactions were performed under stirring in a 1-mL cell in contact with the electrode, while the temperature was maintained at 20 ± 0.1 °C. The concentrations of substrates and enzyme were kept constant and that of hydrogen peroxide varied exactly as used in the experiments in which ϵ_{mix} was determined.

HPLC Analysis of the Phenol Oxidation Products. The reaction mixtures for HPLC analysis of the oxidation products of **1** and **3** contained *p*-cresol 3.2 mM, H_2O_2 0.4 mM, HRP 16 nM or CPO 18 nM, and (*p*-hydroxyphenyl)propionic acid 2.5 mM, H_2O_2 0.5 mM, HRP 42 nM or CPO 38 nM in a total volume of 2 mL of phosphate buffer, pH 5.0. After a 2-min reaction time, the mixtures were extracted twice with diethyl ether (1.5 mL) and twice with ethyl acetate (1.5 mL). The organic phases were evaporated and the residues dissolved in the eluent used in the HPLC analysis. The reaction mixture for HPLC analysis of the oxidation products of **9** contained *N*-acetyltyramine 6.0 mM, H_2O_2 1.6 mM, and HRP 25 nM in a total volume of 125 mL of water. The pH was adjusted to 5.0 by adding small quantities of acetic acid. After 2 min, the reaction mixture was taken to dryness under vacuum at room temperature and the solid residue extracted twice with 2 mL of methanol. The organic phase was evaporated under vacuum, and the residue was dissolved in the eluent used in the analysis. The solutions were analyzed by reverse-phase HPLC on a Merk Lichrosorb RP-18 cartridge. The analysis of the reaction mixture obtained from *p*-cresol was carried out isocratically using a MeOH/H_2O mixture (70:30 v/v) as eluent. The products of oxidation of (*p*-hydroxyphenyl)-propionic acid were analyzed with pure *i*-PrOH and those of the *N*-acetyltyramine oxidation with a *i*-PrOH/MeCN mixture (15:85 v/v). The HPLC detector was set at 290 nm. The HPLC chromatograms from CPO and HRP reactions were identical. For the reactions of **1** and **9**, three peaks with retention times of 4.6, 7.1, and 8.6 min (with a 0.8 mL/min flow rate of the eluent) and 4.3, 7.1, and 10.2 min (flow rate 0.7 mL/min) were observed, respectively. For the oxidation of **3**, only two peaks were observed in different conditions (e.g., retention times of 3.8 and 5.5 min with flow rate 0.7 mL/min). The oxidation products of *N*-acetyltyramine were also isolated on a Supelco RP-18 semipreparative column using *i*-PrOH/MeCN (25:75 v/v) as eluent. In this case, the material from the crude reaction mixture was dissolved in *i*-PrOH to obtain sufficiently high concentrations.

Spectral Measurements. Spectral changes during the reaction of enzyme intermediates and *p*-cresol were observed in the same apparatus used for kinetic measurements but at 8.0 °C. The enzyme (5.0 μM) and *p*-cresol (1.0 mM) were incubated for 10 min in acetate buffer, pH 5.0. Hydrogen peroxide (1.0 mM final concentration) was added under stirring, and several spectra were recorded at 0.3-s intervals in the range 300–500 nm.

Table 1: Difference Spectra Characteristics and Apparent Binding Constants of CPO–Phenol Complexes in Acetate Buffer, pH 5.0, at 23 °C

substrate	λ_{min} (nm)	$\Delta\epsilon_\infty$ (M^{-1} cm^{-1})[a]	K_B (mM^{-1})	n[b]
1	424	7000	0.12	1.02
2	430	3300	0.04	1.06
3	424	3500	0.09	1.00

[a] $\Delta\epsilon$ values calculated from the extrapolated ΔA_∞. [b] Hill coefficient.

Substrate-Binding Experiments. The equilibrium constants for the binding of **1**, **2**, and **3** to CPO were determined by spectrophotometric titrations at 20 ± 0.1 °C using an HP 8452A diode array spectrophotometer. A few microliters of concentrated substrate solutions (~50 mM) in 100 mM acetate buffer, pH 5.0, was added to a 1-mL solution of CPO in the same buffer. Difference spectra of enzyme–substrate versus enzyme were recorded after a few minutes of incubation.

The binding constants were obtained by double-reciprocal plots of absorbance against substrate concentration, and the stoichiometry of the complex was established by Hill plots as described previously (Casella et al., 1991). The dilution of the solution which follows the addition of the titrant was taken into account, while correction of the actual concentration of unbound ligand in solution was not necessary. The K_B obtained for **1–3** are reported in Table 1. Titrations of CPO with **5**, L-**7**, **9**, and L-**12** led to irregular changes in the Soret spectrum, and it was not possible to obtain reliable values for K_B.

NMR Measurements. All proton NMR measurements were performed on Bruker AC-200 and AM-500 spectrometers using a 5-mm probe. The enzyme samples were prepared by ultrafiltration and repeated exchange with 0.1 M deuterated acetate buffer, pH 5.0 (uncorrected for the small isotope effect). The enzyme concentration was 0.5 mM. The substrates were added directly in the NMR tube as concentrated solutions in D_2O. At least 10.000–40.000 transients were accumulated over 40 kHz using 16K data points. The residual HDO signal was presaturated for 1 s before the acquisition pulse. A line-broadening function of 50 Hz was applied before Fourier transformation. The chemical shifts are referred to the residual HDO signal (4.7 ppm).

Relaxation Rate Measurements. Titrations of the substrates with the enzyme were carried out by adding small volumes of the enzyme solutions (~10^{-4} M) to 400 μL of the phenol solution (~100 mM). Solutions of **1–3**, **9**, and L-**12** were prepared in 0.1 M deuterated acetate buffer, pH 5.0, while those of **5** and L-**7** were prepared in 0.2 M deuterated acetic acid, and NaOD was added to reach pH 5.0 (uncorrected for the small isotope effect). The temperature was calibrated using Bruker standard solutions and controlled by the control unit of the instrument with a precision of ±1 °C. Longitudinal relaxation times were determined at 200 MHz using the standard inversion recovery method, while the Carr–Purcell–Meilboom–Gill pulse sequence was used to obtain the transverse relaxation times (Martin et al., 1979). From the values of $T_{i,obs}$ (i = 1, 2), it is possible to calculate T_{ib}, which is the T_i for the bound substrate when this is in fast exchange between the active site and the bulk solution, from the equation:

$$\frac{1}{T_{i,\text{obs}}} = \left[\frac{1}{T_{ib}} - \frac{1}{T_{if}}\right]\frac{E_0}{K_D + S_0} + \frac{1}{T_{if}} \quad (1)$$

the limitations of which have already been discussed (Casella et al., 1992). In this equation, T_{if} is the T_i for the free substrate, E_0 and S_0 are the initial enzyme and substrate concentrations, respectively, and K_D is the dissociation constant for the enzyme–substrate complex (K_B^{-1}). K_D values for **1–3** were obtained from the spectrophotometric titrations described before. K_D values estimated from T_1 measurements for the same substrates, using the ratio intercept/slope of the reciprocal relaxation rate change versus bulk substrate concentration plot, were in good agreement with those in Table 1. As we already explained in the substrate-binding studies, the evaluation of the K_B from the spectrophotometric titrations was impossible for **5**, L-**7**, **9**, and L-**12**. The changes in the relaxation rates of the protons of these compounds after the addition of CPO are very small, and therefore, the K_B data are inaccurate due to the large distances of the bound phenols from the paramagnetic center. To obtain indicative values of the proton–heme distances, we used two values of K_B: 0.100 and 0.010 mM^{-1}, which are reasonable upper and lower limits for this parameter.

For **1**, the measurements were done at different temperatures, in the range 5–30 °C, to check if the time for the chemical exchange can interfere in the evaluation of T_{iM}, the paramagnetic component of the relaxation (Casella et al., 1992). If τ_M is negligible, T_{ib} is equal to T_{iM}, from which it is possible to calculate the distances of the substrate protons from the paramagnetic center according to the Solomon–Bloembergen equations (Solomon, 1955; Bloembergen, 1957) which, simplified for the extreme narrowing conditions, give

$$r\,(\text{cm}) = [(8.66 \times 10^{-31})T_{1M}\tau_c]^{1/6} \quad (2)$$

The value of τ_c for CPO, necessary for obtaining the values of the distances, was previously reported by us (Casella et al., 1992) and equal to 8.8×10^{-11} s.

RESULTS

Kinetic Studies, Substrate Effects, and Analysis of the Products. An initial screening of CPO reactivity toward the phenolic compounds reported in Figure 1 showed that all the molecules bearing free amino groups on the side chain (**4**, **5**, **7**, **8**) or branching at the carbon atom adjacent to the phenol nucleus (**6**, **11**) were unaffected by the enzyme in the presence of hydrogen peroxide. By contrast, all the compounds in Figure 1 are substrates for HRP in the same conditions. On the other hand, the CPO reactivity could be restored in some cases when the amino group was *N*-acetylated (**9**, **10**, L-**12**) but not in others (D-**12**, L-**11**, D-**11**).

A kinetic study of the CPO-catalyzed reactions in the presence of hydrogen peroxide shows that the oxidation of phenols occurs with classical substrate saturation behavior. In the case of the more reactive phenols (**1–3**), substrate inhibition was observed at high substrate concentrations (above ~30 mM) (Figure 2). A similar effect was noted in the CPO-catalyzed peroxidation of catechol (Libby et al., 1989). The kinetic measurements were then performed at substrate concentrations lower than those causing inhibition. For the other substrates, **9** and L-**12**, the inhibition effect was not observed, probably because the substrate concentrations needed are much higher than their solubility. The primary kinetic data were converted in units of mol/time by using an apparent ϵ_{mix}, reflecting the product composition, which was conveniently determined from analysis of the HRP-catalyzed

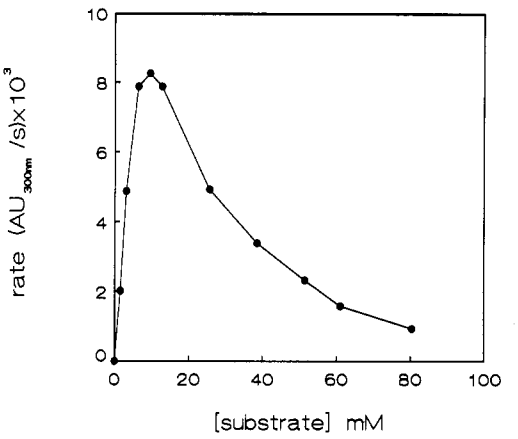

FIGURE 2: Plot of rate versus substrate concentration showing substrate inhibition for the CPO-catalyzed oxidation of *p*-hydroxyphenylacetic acid.

oxidations. Using CPO as catalyst, the same UV bands, with identical λ_{max} and shape, for the products as in the HRP-catalyzed oxidations develop during the reaction. But the values of ϵ_{mix} calculated in the same conditions (H_2O_2 limiting reagent) are significantly smaller, particularly with the less reactive substrates, because the parallel catalatic activity of CPO consumes part of the oxidant. Actually, taking into account the amount of hydrogen peroxide dismutated, through the measurement of the dioxygen evolved in the catalatic reaction, we obtained corrected ϵ_{mix} values for the CPO-catalyzed reactions which are within ±10% of those reported above for the HRP-catalyzed reactions (data not shown).

The HPLC analyses of the reaction mixtures from the enzyme-catalyzed oxidations of **1**, **3**, and **9** were identical using HRP or CPO. The three peaks observed in the chromatograms of the mixtures from the oxidation of **1** and **9** are attributed to unreacted phenol and the two products of oxidative coupling, **13** and **14**, respectively, in order of

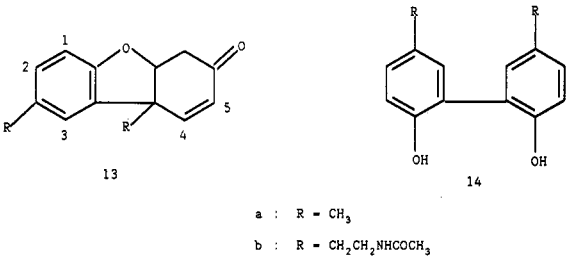

increasing retention time. The products **13a** and **14a** were identified by comparison with the data reported previously (Hewson & Dunford, 1976; Pietikäinen & Adlercrentz, 1990), while **13b** and **14b** were isolated on a semipreparative column and their structure assigned by analysis of their NMR spectra (Figure 3). The assignments were confirmed by COSY experiments. The two peaks in the HPLC chromatogram of the reaction mixture from oxidation of **3** are assigned to excess phenol and one or, more probably, the nonseparable mixture of the two dimeric oxidative coupling products, in order of increasing retention time.

The oxidation of phenols by H_2O_2 catalyzed by peroxidases usually follows this scheme (Dunford & Stillman, 1976; Frew & Jones, 1984):

$$\text{(a)}\quad E + H_2O_2 \rightleftarrows (E\text{–}H_2O_2) \rightarrow E\text{–}I + H_2O \quad (3)$$

binding of H_2O_2 and formation of compound I

(b) E–I + phenol ⇄ (E–I–phenol) → E–II + (phenol)• binding of the phenol to compound I, one-electron oxidation of the phenol, and formation of compound II (4)

(c) E–II + phenol ⇄ (E–II–phenol) → E + (phenol)• (5) binding of the phenol to compound II, one-electron oxidation, and reestablishment of resting enzyme

If the rate of the two last steps is very different, the scheme can be reduced to the following:

$$E + H_2O_2 \rightleftarrows (E\text{–}H_2O_2) \rightarrow E_{ox} \quad (6)$$

$$E_{ox} + \text{phenol} \rightleftarrows (E_{ox}\text{–phenol}) \rightarrow E + \text{products} \quad (7)$$

In the case of HRP catalysis, step c is rate limiting and E_{ox} represents compound II (Hewson & Dunford, 1976a,b; Critchlow & Dunford, 1972). This was also proved here by performing experiments in which the slow intermediate could be spectrally identified. The same is not true in the case of CPO catalysis because, as shown by spectral experiments, both compound I and II are present during enzyme turnover (Figure 4). The amount of compound II during turnover, for instance, is much larger in the CPO-catalyzed oxidation of ascorbic acid [compare Figure 4 here with Figure 1 in Thomas et al. (1970b)]. This indicates that the difference in the rates of steps b and c is not as high as that for HRP. The need of using rapid scan techniques prevents a more detailed kinetic study at this stage; however, the little difference in the rates of steps b and c was shown by the kinetics of the CPO-catalyzed oxidation of *p*-phenolsulfonic acid (Lambeir et al., 1987).

In spite of the above limitations, for both the HRP and CPO reactions, the scheme can be reduced to a simple bimolecular ping-pong mechanism (Cleland, 1963). The resulting rate equation from this treatment is

$$v = \frac{V_{max}}{1 + \frac{K_{M(H_2O_2)}}{[H_2O_2]} + \frac{K_{M(phenol)}}{[phenol]}} \quad (8)$$

The only difference for the two enzymes is that $K_{M(phenol)}$ contains terms which refer only to the last step (eq 5) in the case of HRP, while it contains terms of both steps b and c in the case of CPO.

Referring to eq 8, in order to analyze the primary kinetic data with a Michaelis–Menten equation, the term $K_{M(H_2O_2)}/[H_2O_2]$ must be negligible. This condition is fulfilled when the hydrogen peroxide concentration is high enough to saturate the enzyme. In these conditions, the catalatic activity can be neglected. By performing kinetic studies varying the H_2O_2 concentration and keeping fixed that (saturating) of the substrate, the value of $K_{M(H_2O_2)}$ can be determined. This depends on which substrate is used to saturate the enzyme, and for CPO, we found that the lowest affinity for H_2O_2 was exhibited by the enzyme in the presence of the most reactive phenol. The following values were obtained. $K_{M(H_2O_2)}$ in the presence of *p*-cresol = 6.6 mM; $K_{M(H_2O_2)}$ in the presence of *p*-hydroxyphenylacetic acid = 2.8 mM; $K_{M(H_2O_2)}$ in the presence of (*p*-hydroxyphenyl)propionic acid = 1.4 mM. Although these values are clearly overestimates because it would be necessary to determine for every experiment the contribution of the catalatic activity consuming H_2O_2, the correlation between $K_{M(H_2O_2)}$ and reactivity of the phenol suggests a competition between the substrate and hydrogen peroxide for the active site. This is confirmed by the substrate inhibition effect noted earlier. The $K_{M(H_2O_2)}$ values found here are, however, in the same range as those found for $K_{M(H_2O_2)}$ in the presence of pyrogallol (4.3 mM) (McCarty & White, 1983) and monochlorodimedone (0.8 mM) (Hager et al., 1966).

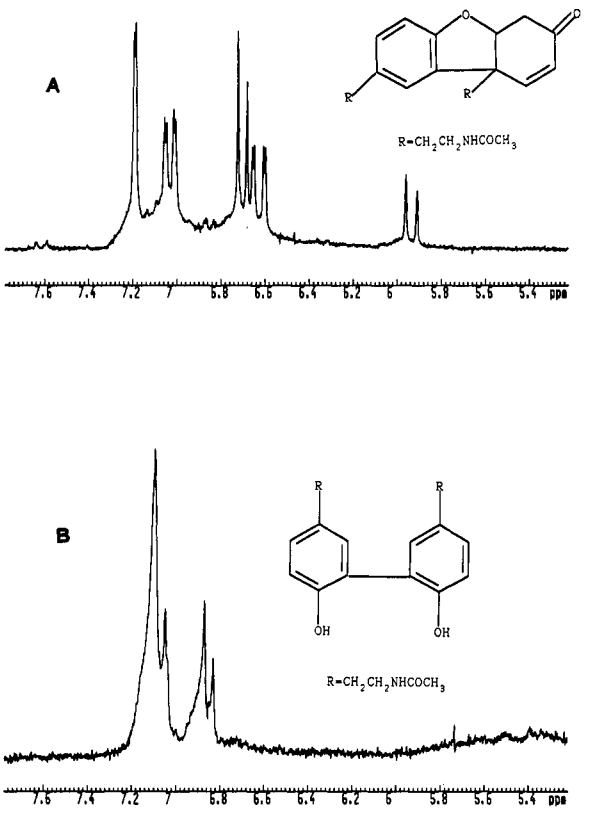

FIGURE 3: 200-MHz ^{1}H-NMR spectra of the products **13b** (A) and **14b** (B). Only the low-field region of the spectra is shown because the aliphatic region is contaminated by some peaks due to material released from the HPLC column.

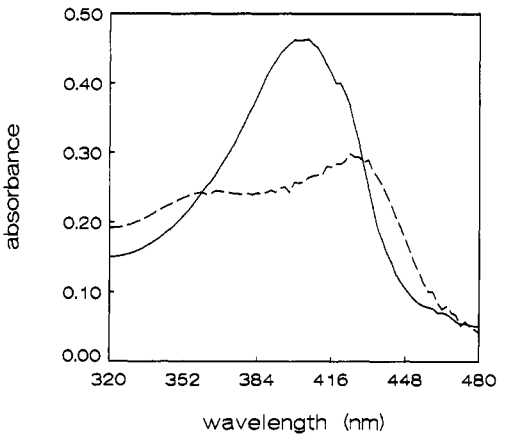

FIGURE 4: Soret spectra of CPO (2.9 μM) and *p*-cresol (1.07 mM) in acetate buffer, pH 5.0, before (—) and after (- - -) the addition of hydrogen peroxide (1.9 mM) (turnover conditions).

Once the conditions of hydrogen peroxide saturation were set for the various substrates and the ϵ_{mix} calculated, the kinetic data could be analyzed with the Michaelis–Menten scheme. The data are reported in Table 2, where the enzymatic activity is given in terms of k_{cat}, the turnover number.

Paramagnetic NMR Spectra and Relaxation Rate Measurements.[2] The ^{1}H-NMR spectra of native CPO and CPO

[2] The authors thank Ada Manzocchi of the Dipartimento di Chimica e Biochimica Medica, University of Milano, for the ^{1}H-NMR spectra at 500 MHz.

Table 2: Kinetic Parameters for CPO- and HRP-Catalyzed Oxidation of Phenols by Hydrogen Peroxide in 0.1 M Acetate Buffer, pH 5.0

substrate	k_{cat} (s^{-1})	K_M (mM)	k_{cat}/K_m (M^{-1} s^{-1})
		CPO	
1[a]	2700	10.6	2.52×10^5
2[b]	500	48.4	1.00×10^4
3[c]	350	84.5	4.08×10^3
9[c]	370	50.2	7.45×10^3
L-**12**[c]	0.4	96.2	3.60
		HRP[d]	
1	860	2.9	2.94×10^5
2	630	6.2	1.02×10^5
3	200	7.2	2.78×10^4
9	1850	2.5	7.55×10^5
L-**12**	450	31.4	1.44×10^4
D-**12**	320	54.3	5.85×10^3

[a] $[H_2O_2]$ = 5.0 mM. [b] $[H_2O_2]$ = 1.0 mM. [c] $[H_2O_2]$ = 0.5 mM. [d] $[H_2O_2]$ = 0.4 mM.

in the presence of 10 or 50 mol equiv of *p*-cresol show marked differences, while the addition of tyramine causes no significant effect in the spectrum of the enzyme (Figure 5). The paramagnetic spectrum of CPO in the region 40–80 ppm consists of a pattern of eight signals (68.9, 64.3, 58.6, 55.7, 48.0, 47.2, 40.9, 40.8 ppm), which resemble two sets of four split signals and are attributed to the heme methyls (Goff et al., 1985). It has been recently shown that the splitting is due to the presence of the two different isoenzymes rather than to heme disorder (Dugat et al., 1992). The addition of *p*-cresol broadens remarkably the four downfield signals and the other signals between 20 and 40 ppm until they almost disappear, indicating that the system is undergoing an intermediate chemical exchange; the two pairs of overlapping peaks at 47.2 and 48.0, and 40.8 and 40.9 ppm merge into broad signals which are shifted to 50.1 and 42.1 ppm (Figure 5, top).

The extent of the broadening is different depending on the field: indeed, while at 500 MHz the downfield peaks almost disappear, at 200 MHz a new broad resonance at 64.5 ppm can be observed. This signal sharpens on raising the temperature to 308 K, while another resonance at 77 ppm can be observed (Figure 5, bottom).

Measurements of the proton longitudinal (T_1) and transverse (T_2) relaxation times of **1**–**3**, **5**, L-**7**, **9**, and L-**12** were performed in the presence of increasing amounts of CPO. Figure 6 shows, for the different proton resonances of *p*-cresol, the experimental results obtained in the titration with CPO as plots of $(T_{1obs})^{-1}$ or $(T_{2obs})^{-1}$ versus $E_0/(K_D + S_0)$. Straight lines have also been obtained for all proton signals of the other substrates investigated in similar titration experiments. The values of T_{1B} and T_{2B} so obtained are listed in Table 3.

The ratio T_{1B}/T_{2B} should be 1.17 in the extreme narrowing condition, as is usually the case for high-spin hemoproteins, but clearly, the values we obtained here for substrates **1**, **5**, **7**, and **9** are much higher, ranging from 10 to 20. This means that a second effect, different from that of paramagnetic dipolar coupling, is active on T_2. This effect could be a small contact contribution, a Curie spin electron relaxation contribution or, more probably, a limitation due to τ_M (the time for the chemical exchange) (Bertini & Luchinat, 1986). From the temperature dependence of $(T_{1B})^{-1}$ and $(T_{2B})^{-1}$, one can decide which mechanism is operative. The experimental values of $(T_{1B})^{-1}$ and $(T_{2B})^{-1}$ for **1** at different temperatures show an increase for the first and a marked decrease for the second on decreasing the temperature. This indicates an intermediate chemical exchange regime, as was noted previously in the paramagnetic spectrum of the complex CPO–*p*-cresol. In this regime, $(T_{2B})^{-1}$ is influenced by τ_M, while $(T_{1B})^{-1}$ is not. In fact, from a plot of $(T_{1B})^{-1}$ versus T^{-1}, the parameter $\Delta G^{\ddagger}$ = 9.2 kJ mol^{-1} was obtained; this indicates that the activation energy is basically due to diffusion processes. $(T_{1B})^{-1}$ can then be interpreted as $(T_{1M})^{-1}$, i.e., it is entirely determined by the paramagnetic dipolar coupling. Owing to the problem of chemical exchange, which is not fast enough, as it occurred previously in the case of sulfides binding to CPO (Casella et al., 1992), a direct measurement of τ_c through the ratio T_{2M}/T_{1M} was not possible. To get structural information on the

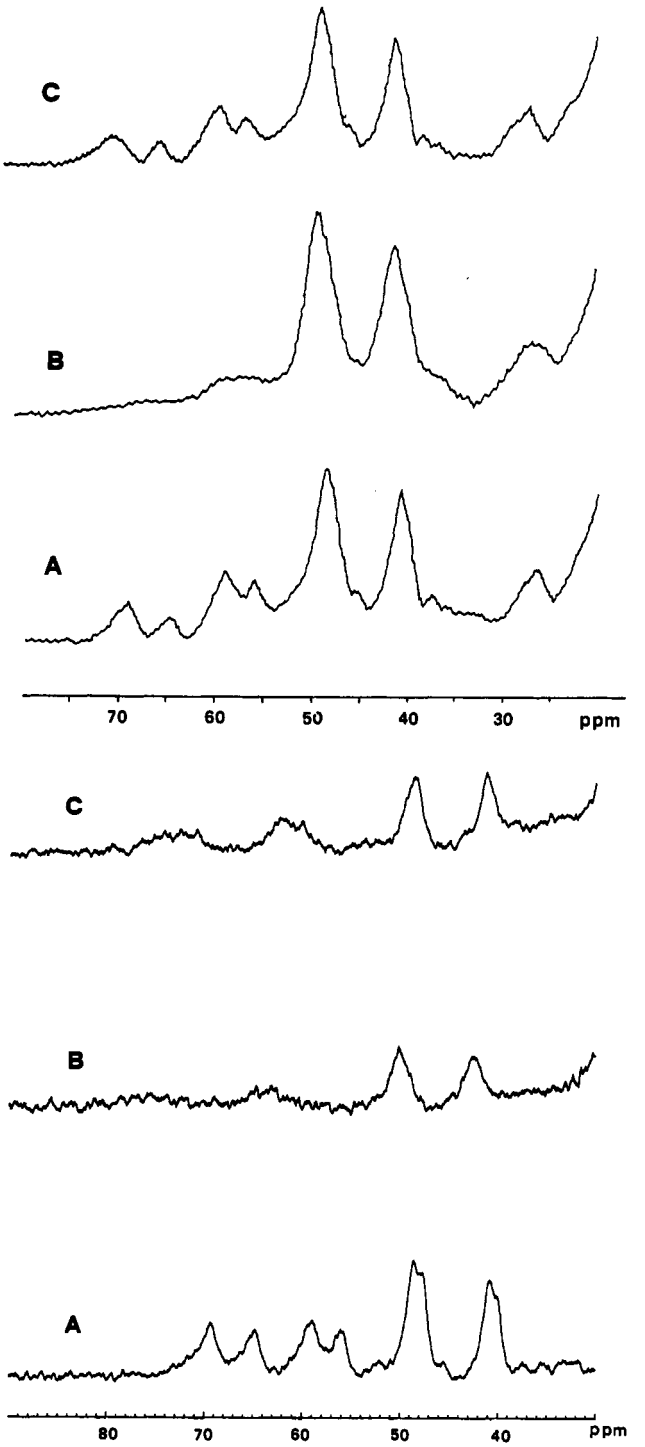

FIGURE 5: (Top) Proton NMR spectra at 500 MHz of (A) CPO (0.5 mM, acetate buffer in D_2O, pD 5.0) and the enzyme after the addition of 10 mol equiv of *p*-cresol (B) or tyramine (C). (Bottom) Proton NMR spectra at 200 MHz of (A) CPO (0.5 mM, acetate buffer in D_2O, pD 5.0) at 298 K and the enzyme after the addition of 10 mol equiv of *p*-cresol at 298 K (B) and at 308 K (C).

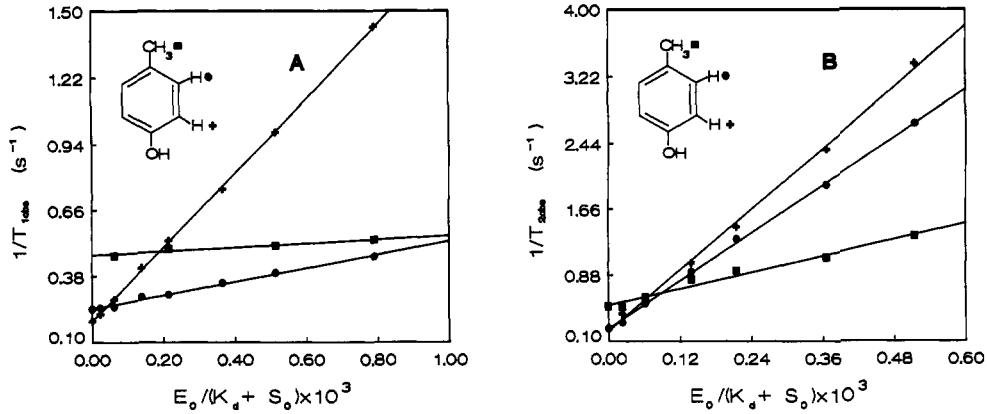

FIGURE 6: Plots of $1/T_{1obs}$ versus fraction of bound ligand (A) and $1/T_{2obs}$ versus fraction of bound ligand (B) for the protons of *p*-cresol in the presence of CPO.

Table 3: Relaxation Times for the Protons of Phenols Bound to CPO

substrate	T (K)	proton	T_{1B} (s)[a]	T_{2B} (s)[a]
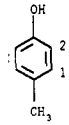	278	1	2.1×10^{-3}	
		2	4.6×10^{-4}	
		$-CH_3$	8.4×10^{-3}	
	288	1	3.0×10^{-3}	
		2	5.6×10^{-4}	
		$-CH_3$	1.9×10^{-4}	
	295	1	3.5×10^{-3}	2.4×10^{-4}
		2	7.2×10^{-4}	1.7×10^{-4}
		$-CH_3$	1.4×10^{-2}	7.4×10^{-4}
	300	1		1.5×10^{-4}
		2		7.8×10^{-5}
		$-CH_3$		2.2×10^{-4}
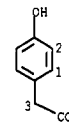	295	1	3.0×10^{-3}	
		2	8.8×10^{-4}	
		3	7.3×10^{-3}	
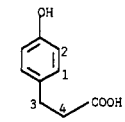	295	1	5.4×10^{-3}	
		2	7.5×10^{-4}	
		3	1.0×10^{-2}	
		4	6.4×10^{-3}	
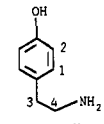	295	1	7.9×10^{-2} (2.1×10^{-2})	5.7×10^{-3} (1.5×10^{-3})
		2	6.7×10^{-2} (2.1×10^{-2})	5.6×10^{-3} (1.5×10^{-3})
		3	1.9×10^{-2} (5.2×10^{-3})	2.9×10^{-3} (8.0×10^{-4})
		4	2.8×10^{-2} (7.7×10^{-3})	3.2×10^{-3} (8.9×10^{-4})
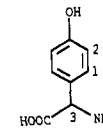	295	1	8.3×10^{-2} (2.1×10^{-3})	7.6×10^{-3} (2.1×10^{-3})
		2	8.2×10^{-2} (2.6×10^{-3})	9.4×10^{-3} (2.6×10^{-3})
		3	$\sim 4 \times 10^{-2}$ ($\sim 10^{-2}$)	5.1×10^{-3} (1.4×10^{-3})
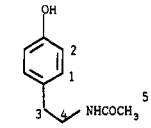	295	1	4.0×10^{-2} (1.0×10^{-2})	2.2×10^{-3} (5.8×10^{-4})
		2	5.9×10^{-3} (1.5×10^{-3})	1.7×10^{-3} (4.7×10^{-4})
		3	5.8×10^{-2} (1.5×10^{-2})	9.4×10^{-3} (2.5×10^{-3})
		4	6.0×10^{-2} (1.2×10^{-2})	6.1×10^{-3} (1.6×10^{-3})
		5		6.5×10^{-3} (1.7×10^{-3})

[a] The data for T_{1B} (s) and T_{2B} (s) were calculated assuming $K_B = 0.10$ mM^{-1}; in parentheses are the data obtained with $K_B = 0.010$ mM^{-1}.

binding of phenols to CPO, we thus used the value of τ_c measured previously from the line width of the heme methyl protons (Casella et al., 1992), whose distances from the paramagnetic center are known (620 pm). The resulting iron–proton distances for the bound substrates expressed in angstroms are shown in Figure 7. We can distinguish two different binding modes: substrates **1–3** and **9** bind close to the heme, with the phenol groups facing the iron atom and the aromatic ring inclined with respect to the heme plane, and donor molecules **5** and L-**7**, which contain free amino groups, bind at larger distances from the heme, with the phenol group pointing somewhat away from the iron.

DISCUSSION

Chloroperoxidase is considered less efficient than other peroxidases, e.g., horseradish peroxidase, in common peroxidatic reactions (Lambeir et al., 1987). This is certainly true in many cases, but rather than due to an intrinsic limitation of the oxidizing power of its catalytic intermediates, the low efficiency of CPO as a peroxidatic enzyme seems more related

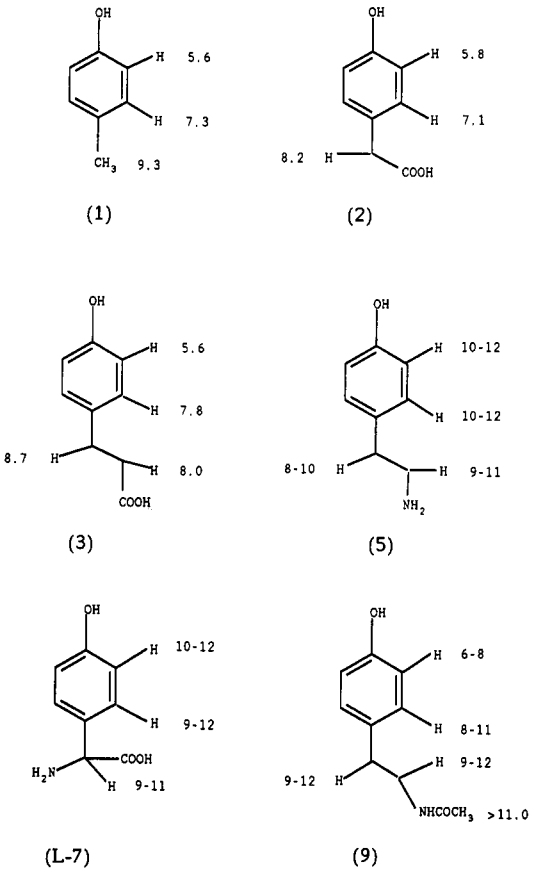

FIGURE 7: Iron–proton distances (Å) for CPO–phenol complexes derived from relaxation time measurements. The upper estimated uncertainties in the calculated distances are ±10%.

to restrictions in the access or less favorable disposition of substrates in the active site. In fact, it has been estimated that the redox potential of CPO compound I must be greater than that of HRP and lignin peroxidase (Sarkanen et al., 1991; Renganathan et al., 1987). On the other hand, CPO is much more selective toward substrates than the other members of the peroxidase family.

Selectivity toward phenolic substrates operates through size, excluding potential substrates containing bulky substituents, particularly those with branching at the carbon atom connected with the phenol nucleus, and through charge, excluding positively charged molecules such as the phenolic amines. These results agree with previous ligand-binding studies to the heme iron of CPO performed by Sono et al. (1986), where it was found that neutralization of the negative charge of small ligand anions, either by binding of their protonated form (for weakly acidic ligands) or upon binding to the enzyme protonated form (for strongly acidic ligands), is essential for entering the "gate" of the CPO active site. It is also significant that of the two optical isomers of *N*-acetyltyrosine, only the L form can act as a substrate. This enantiospecificity requires recognition of the relative spatial orientation of the substituents at the amino acid α carbon atom and thus the existence of a complementary couple of polar protein residues in the active-site pocket or access channel of CPO suitable for the L form. For HRP and LPO, there is some preference in the binding of chiral tyrosine derivatives (Casella et al., 1991), but this does not prevent both of them to act as substrates for the enzymes. This suggests some rigidity in the active-site cleft of CPO. Somewhat strict steric requirements are in fact imposed by this enzyme also in the binding of aromatic sulfides (Casella et al., 1992). In that case, the active-site topology

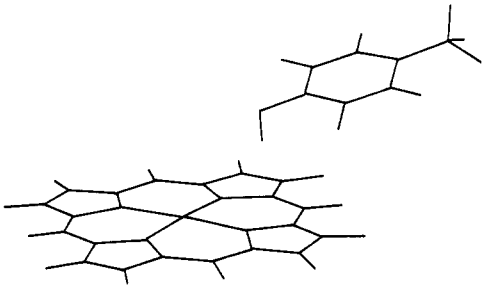

FIGURE 8: Molecular models showing the relative heme–*p*-cresol disposition in the CPO active site deduced from NMR relaxation rate measurements. The phenol nucleus is depicted above the meso edge because the δ-meso edge is known to be exposed (Samokyszyn & Ortiz de Montellano, 1991).

could be fitted by substrates structurally related to methyl *p*-tolyl sulfide, which can be compared with *p*-cresol here, and substrate immobilization led to remarkable enantioselectivity in the sulfoxidation reaction (Colonna et al., 1990, 1992). A linear chain substituent *para* to the sulfur atom was tolerated, particularly when containing polar groups, as it is here with the acidic phenols and *N*-acetyltyramine. But replacement of the *para* substitution pattern with *ortho* substitution led to a drop in affinity *and* reactivity of the sulfides (Casella et al., 1992; Colonna et al., 1990, 1992). This behavior seems to parallel the exclusion of phenols with branching at the carbon atom attached to the aromatic nucleus that we observe here, as if the access to the CPO active site were controlled by a channel of limited diameter.

The lack of reactivity of phenols carrying amino groups in the side-chain substituent may be related to the fact that the distal heme pocket of CPO contains an excess of positive charge. The charge carried by the distal histidine (His-38) (Blanke & Hager, 1990), an arginine (Dugad et al., 1992), and possibly other residues in the vicinity of the heme may not be counterbalanced by negatively charged residues, and this may prevent the approach of phenolic amines to a suitable distance or disposition from the heme for productive electron transfer to occur. Support for this view comes from the differences in the iron–proton distances that we can estimate, e.g., for bound tyramine and *N*-acetyltyramine to CPO (Figure 7), which are beyond the limited accuracy of the data. Binding of *N*-acetyltyramine to CPO occurs, like for the other reactive phenols **1–3**, with the aromatic nucleus closer to the iron, while for bound tyramine or tyrosine, the phenol nucleus is more distant than the aliphatic chain from the iron and is probably even outside the active-site cavity. This result is very important because it correlates the reactivity of the enzyme uniquely to a suitable disposition of the substrate in the active-site pocket. It is unfortunate that the inactivity of CPO in basic medium prevents investigation of whether the enzyme can become active toward the phenolic amines in conditions where these compounds lack their positive charge.

The iron–proton distances determined for the CPO complexes with phenols **1–3** and **9** can only be accounted for by a disposition of these substrates above the heme plane, since some of the distances are too short for a disposition near the heme edge, as found for the binding of phenolic substrates to other peroxidases such as HRP or LPO (Sakurada et al., 1986; Modi et al., 1989b; Casella et al., 1991) (Figure 8). This result is consistent with a large body of evidence indicating that substrates have access to the heme iron and the ferryl oxygen of CPO. This is shown by the formation of a phenyl–iron complex by reaction with phenylhydrazine (Samokyszyn & Ortiz de Montellano, 1991) and by oxygen incorporation

into the product in the epoxidation of styrene (Ortiz de Montellano et al., 1987), the *N*-oxidation of arylamines (Doerge & Corbett, 1991), and the sulfoxidation of thioanisoles (Kobayashi et al., 1986). Our previous studies on CPO–sulfide complexes also agreed with this view, but the iron–proton distances estimated through NMR relaxation rate measurements were larger than those found here. The differences do not arise from an influence of the mixed aqueous–organic solvent that had to be used in the case of sulfides, since we have found that for *p*-cresol the relaxation rates in the presence of CPO are identical in (deuterated) aqueous buffer and aqueous buffer–acetone (75/25 v/v) medium. The close approach to the heme attainable by *p*-cresol can explain the unusual observation that its addition to CPO causes the broadening of some of the heme NMR signals (Figure 5).

The smaller effects undergone by the two intense heme methyl signals on *p*-cresol binding indicate these are associated with groups which are more buried within the protein cavity and are much less affected by the presence of the substrate. The same downfield heme signals underwent smaller changes on binding aromatic sulfides to CPO compared with the other heme signals, even though the latter did not exhibit the marked broadening effects observed here. The field dependence of the broadening is as we expect for an exchange process that is not in the fast regime and confirms what was suggested by the T_{1B}/T_{2B} ratio. Indeed, the relaxation measurements show that the bound lifetime was in the order of 10^{-3}–10^{-4} s. From the value of K_B, it can be estimated that about 50% of the enzyme is in the bound state in the experiments reported in Figure 5. This means that the signal at 64.5 ppm should be the average of two almost equally populated sites, one of which is at 60 ppm (the signal for the free enzyme). Therefore, the signal of the bound enzyme is expected to be at about 10 ppm downfield. This clearly demonstrates that the complex has to still be high spin and the phenol does not directly coordinate to the iron center, thus experiencing only dipolar paramagnetic contributions. The chemical shift differences are expected to be smaller for the free and bound *p*-cresol than those for the free and *p*-cresol-bound CPO; this explains why an average signal can be observed for the substrate.

In conclusion, the present investigation confirms that the active-site structure of CPO is different from those of classical peroxidases. Although the nature of the residues surrounding the heme in the distal region is probably similar (Blanke & Hager, 1990; Dugad et al., 1992), the CPO site is more open above the heme, and this enables the enzyme to perform peroxygenative reactions in much the same way as P-450 performs monooxygenase reactions. In this respect, it is interesting to note that the iron–proton distances that have been recently determined for substrates bound to P-450 (6–9 Å) (Castro-Maderal & Sullivan, 1992) are similar to those we find here for CPO–phenol complexes. On the other hand, the size of the pocket and/or the access channel to the substrate-binding region is limited, and this originates marked selectivity effects and substrate recognition that are unknown among common peroxidases. The arrangement of substrates above the heme, however, may be less productive when CPO acts as a peroxidase. Single-electron transfers from the phenols to the heme during the catalytic cycle might be less favorable with this disposition than, as with common peroxidases, when the substrates bind near the heme edge, where π-orbital overlap between the porphyrin and the aromatic ring of the substrate is possible. We may even raise the question of why CPO does not effect an oxygen-transfer reaction to a CH group of the phenol nucleus, since, for instance, like P-450 it is able to catalyze the epoxidation of unsaturated substrates (Ortiz de Montellano et al., 1987; Colonna et al., 1993; Allain et al., 1993). The peroxygenase pathway is certainly disfavored for kinetic reasons, since the oxygen-transfer reaction of CPO to, e.g., styrenes is much slower than the phenol radical coupling reaction studied here,[3] and for steric reasons because from the picture emerging for the CPO–phenol complexes, the substrate ring CH groups cannot be lined up with the Fe=O bond and appear actually much closer to the meso edge (Figure 8). In addition, phenols are the products of oxidation of aromatic compounds by P-450s (Guengerich & Macdonald, 1990; Ortiz de Montellano, 1986) and are generally not considered as substrates for the heme monooxygenases. Reports on the oxidation of phenolic compounds by microsomal fractions of plant extracts show that both radical coupling reactions (Zenk et al., 1989) and phenol ring hydroxylations (Durst, 1989) can occur, the latter with high substrate specificity, depending on the source. However, the attribution of these enzymatic activities to P-450s must await experiments on purified protein samples.

[3] L. Casella, M. Gullotti, S. Poli, and E. Santelli, unpublished observations.

REFERENCES

Allain, E. J., Hager, L. P., Deng, L., & Jacobsen, E. N. (1993) *J. Am. Chem. Soc. 115*, 4415–4416.

Araiso, T., Rutter, R., Palcic, M., Hager, L. P., & Dunford, H. B. (1981) *Can. J. Biochem. 59*, 233–236.

Bayse, G. S., Michaels, A. W., & Morrison, M. (1972) *Biochim. Biophys. Acta 284*, 34–42.

Bertini, I., & Luchinat, C. (1986) in *NMR of Paramagnetic Molecules in Biological Systems* (Lever, A. B. P., & Gray, H. B., Series Eds.) pp 91–94, The Benjamins/Cummings Publishing Co. Inc., Menlo Park, CA.

Blanke, S. R., & Hager, L. P. (1988) *J. Biol. Chem. 263*, 18739–18743.

Blanke, S. R., & Hager, L. P. (1990) *J. Biol. Chem. 265*, 12454–12461.

Bloembergen, N. (1957) *J. Chem. Phys. 27*, 572–573.

Casella, L., Gullotti, M., Poli, S., Bonfà, M., Ferrari, R. P., & Marchesini, A. (1991) *Biochem. J. 279*, 245–250.

Casella, L., Gullotti, M., Ghezzi, R., Beringhelli, T., Colonna, S., & Carrea, G. (1992) *Biochemistry 31*, 9451–9459.

Castro-Maderal, L., & Sullivan, P. D. (1992) *FEBS Lett. 296*, 249–253.

Cleland, W. W. (1963) *Biochim. Biophys. Acta 67*, 104–137.

Colonna, S., Gaggero, N., Manfredi, A., Casella, L., Gullotti, M., Carrea, G., & Pasta, P. (1990) *Biochemistry 29*, 10465–10468.

Colonna, S., Gaggero, N., Casella, L., Carrea, G., & Pasta, P. (1992) *Tetrahedron: Asymmetry 3*, 95–106.

Colonna, S., Gaggero, N., Casella, L., Carrea, G., & Pasta, P. (1993) *Tetrahedron: Asymmetry 4*, 1325–1330.

Critchlow, J. E., & Dunford, H. B. (1972) *J. Biol. Chem. 247*, 3703–3713.

Dawson, J. H. (1988) *Science 240*, 433–439.

Dugad, L. B., Wang, X., Wang, C.-C., Lukat, G. S., & Goff, H. M. (1992) *Biochemistry 31*, 1651–1655.

Dunford, H. B., & Stillman, J. S. (1976) *Coord. Chem. Rev. 19*, 187–251.

Dunford, H. B., & Adeniran, A. J. (1986) *Arch. Biochem. Biophys. 251*, 536–542.

Durst, F. (1989) in *Microbial and Plant Cytochrome P-450: Biochemical Characteristics, Genetic Engineering and Practi-*

cal Implications (Ruckpaul, K., & Rein, H., Eds.) pp 191–232, Akademic Verlag, Berlin.
Frew, J. E., & Jones, P. (1984) *Adv. Inorg. Bioinorg. Mech. 3*, 176–212.
Geigert, J., Lee, T. D., Dalietos, D. J., Hirano, D. S., & Neidleman, S. L. (1986) *Biochem. Biophys. Res. Commun. 136*, 778–782.
Goff, H. M., Gonzaler-Vergara, E., & Bird, M. R. (1985) *Biochemistry 24*, 1007–1013.
Greenstein, J. P., & Winitz, M. (1961) *Chemistry of the Amino Acids*, J. Wiley & Sons, Inc., New York.
Griffin, B. W. in *Peroxidases in Chemistry and Biology* (Everse, J., Everse, K. E., & Grisham, M. B., Eds.) Vol. II, pp 85–137, CRC Press, Boca Raton, FL.
Guengerich, F. P., & Macdonald, T. L. (1990) *FASEB J. 4*, 2453–2459.
Hager, L. P., Morris, D. R., Brown, F. S., & Eberwein, H. (1966) *J. Biol. Chem. 241*, 1769–1777.
Hewson, W. D., & Dunford, H. B. (1976a) *J. Biol. Chem. 251*, 6036–6042.
Hewson, W. D., & Dunford, H. B. (1976b) *J. Biol. Chem. 251*, 6043–6052.
Itahara, T., & Ide, N. (1987) *Chem. Lett.*, 2311–2312.
Itoh, N., Izumi, Y., & Yamada, H. (1987) *Biochemistry 26*, 282–289.
Kobayashi, S., Nakano, M., Goto, T., Kimura, T., & Schaap, A. P. (1986) *Biochem. Biophys. Res. Commun. 135*, 166–171.
Lambeir, A.-M., Dunford, H. B., & PicKard, M. A. (1987) *Eur. J. Biochem. 163*, 123–127.
Libby, R. D., Thomas, J. A., Kaiser, L. W., & Hager, L. P. (1982) *J. Biol. Chem. 257*, 5030–5037.
Libby, R. D., Rotberg, N. S., Emerson, J. T., White, T. C., Yen, G. M., Friedmann, S. H., Sun, N. S., & Goldowski, R. (1989) *J. Biol. Chem. 264*, 15284–15292.
Lukat, G. S., & Goff, H. M. (1986) *J. Biol. Chem. 261*, 16528–16534.
Martin, M. L., Martin, G. S., & Delpuech, J. J. (1979) *Practical NMR Spectroscopy*, pp 283–284, Heyden, London.
McCarthy, M.-B., & White, R. E. (1983) *J. Biol. Chem. 258*, 9153–9158.
Modi, S., Behere, D. V., & Mitra, S. (1989a) *Biochemistry 28*, 4689–4694.
Modi, S., Behere, D. V., & Mitra, S. (1989b) *Biochim. Biophys. Acta 996*, 214–225.
Ortiz de Montellano, P. R., Ed. (1986) *Cytochrome P-450: Structure, Mechanism & Biochemistry*, Plenum Press, New York.
Ortiz de Montellano, P. R., Choe, Y. J., De Pillis, G., & Catalano, C. E. (1987) *J. Biol. Chem. 262*, 11641–11646.
Pietikäinen, P., & Adlercrentz, P. (1990) *Appl. Microbiol. Biotechnol. 33*, 455–458.
Poulos, T. L. (1987) *Adv. Inorg. Biochem. 7*, 1–36.
Renganathan, V., Miki, K., & Gold, M. H. (1987) *Biochemistry 26*, 5127–5132.
Sakurada, J., Takahashi, S., & Hosoya, T. (1986) *J. Biol. Chem. 261*, 9657–9662.
Sakurada, J., Sekiguchi, R., Sato, K., & Hosoya, T. (1990) *Biochemistry 29*, 4093–4098.
Samokyszyn, M. V., & Ortiz de Montellano, P. R. (1991) *Biochemistry 30*, 11646–11653.
Sarkanen, S., Razal, R. A., Piccariello, T., Yamamoto, E., & Lewis, N. G. (1991) *J. Biol. Chem. 266*, 3636–3643.
Solomon, I. (1955) *Physiol. Rev. 99*, 559–565.
Sono, M., Dawson, J. H., Hall, K., & Hager, L. P. (1986) *Biochemistry 25*, 347–356.
Thomas, J. A., Morris, D. R., & Hager, L. P. (1970a) *J. Biol. Chem. 245*, 3129–3134.
Thomas, J. A., Morris, D. R., & Hager, L. P. (1970b) *J. Biol. Chem. 245*, 3135–3142.
Zenk, M. H., Gerardy, R., & Stadler, R. (1989) *J. Chem. Soc., Chem. Commun.* 1725–1727.